

F



\*X2000-00979\*

# DEUTSCHES ELEKTRONEN-SYNCHROTRON



DESY 00-094  
June 2000

## Development of a Pump-Probe Facility with Sub-Picosecond Time Resolution Combining a High-Power Ultraviolet Regenerative FEL Amplifier and a Soft X-Ray SASE FEL

B. Faatz, J. Feldhaus, J. Pflueger, J. Rossbach,  
E. L. Saldin, E. A. Schneidmiller

*Deutsches Elektronen-Synchrotron DESY, Hamburg*

A. A. Fateev, M. V. Yurkov

*Joint Institute for Nuclear Research, Dubna, Moscow Region, Russia*

J. Krzywinski

*Institute of Physics of the Polish Academy of Sciences, Warsaw, Poland*

Eigentum der Property of	<b>DESY</b>	Bibliothek library
Zugang: Accessions:	31. Juli 2000	
Keine Ausleihe Not for loan		

ISSN 0418-9833

NOTKESTRASSE 85 - 22607 HAMBURG

DESY behält sich alle Rechte für den Fall der Schutzrechtserteilung und für die wirtschaftliche Verwertung der in diesem Bericht enthaltenen Informationen vor.

DESY reserves all rights for commercial use of information included in this report, especially in case of filing application for or grant of patents.

To be sure that your preprints are promptly included in the  
HIGH ENERGY PHYSICS INDEX,  
send them to (if possible by air mail):

DESY  
Bibliothek  
Notkestraße 85  
22607 Hamburg  
Germany

DESY-Zeuthen  
Bibliothek  
Platanenallee 6  
15738 Zeuthen  
Germany

## Development of a Pump-Probe Facility with Sub-Picosecond Time Resolution Combining a High-Power Ultraviolet Regenerative FEL Amplifier and a Soft X-ray SASE FEL

B. Faatz<sup>a</sup>, A.A. Fateev<sup>b</sup>, J. Feldhaus<sup>a</sup>, J. Krzywinski<sup>c</sup>, J. Pflueger<sup>a</sup>, J. Rossbach<sup>a</sup>, E.L. Saldin<sup>a</sup>, E.A. Schneidmiller<sup>a</sup> and M.V. Yurkov<sup>b</sup>

<sup>a</sup>Deutsches Elektronen Synchrotron (DESY), 22607 Hamburg, Germany

<sup>b</sup>Joint Institute for Nuclear Research, Dubna, 141980 Moscow Region, Russia

<sup>c</sup>Institute of Physics of the Polish Academy of Sciences, 02688 Warszawa, Poland

### Abstract

This paper presents the conceptual design of a high power radiation source with laser-like characteristics in the ultraviolet spectral range at the TESLA Test Facility (TTF). The concept is based on the generation of radiation in a regenerative FEL amplifier (RAFEL). The RAFEL described in this paper covers a wavelength range of 200–400 nm and provides a 9 MHz train of 200 fs pulses with 2 mJ of optical energy per pulse. The linac operates at 1 % duty factor and the average output radiation power exceeds 100 W. The RAFEL will be driven by the spent electron beam leaving the soft X-ray FEL, thus providing minimal interference between these two devices. After leaving the soft X-ray FEL undulator the electron beam passes another undulator. In this conceptual design we assume to use a planar permanent magnet undulator with 85 periods and a period length of 7 cm. The maximum amplitude of the magnetic field is about 1.4 T. The proposed scheme possesses significant advantages. First, the RAFEL output radiation has the same time structure as the X-ray FEL. Second, the pulses from the RAFEL are naturally synchronized with the soft X-ray pulses from the TTF FEL. Therefore, it should be possible to achieve synchronization close to the duration of the radiation pulses (200 fs) for pump-probe techniques using either an UV pulse as a pump and soft X-ray pulse as a probe, or vice versa, allowing unprecedented insight into the dynamics of electronic excitations, chemical reactions and phase transitions of matter, from atoms, through organic and inorganic molecules and clusters, to surface, solids and plasmas.

### 1 Introduction

The objective of the project is the development of an ultraviolet laser system for pump-probe experiments, in order to exploit the intense soft X-ray pulses from the TTF X-ray FEL [1, 2] for two-color time-resolved measurements down to the level of the pulse width, i.e. to a resolution of a few hundred femtoseconds. Pump-probe techniques using either the soft X-ray FEL pulse as a pump and the UV laser as a probe pulse, or vice versa, promise unprecedented insight into the dynamics of electronic excitations, chemical reactions and phase transitions of matter, from atoms, through organic and inorganic molecules and clusters, to surfaces, solids and plasmas.

The main problem is the development and construction of a synchronized laser system which has the same time structure as the soft X-ray FEL (pulse trains of 800  $\mu$ s duration at 10 Hz, with repetition rate of 9 MHz within a pulse train) and produces short, intense pulses with a width of about 200 fs. In order to provide sufficient flexibility for the users, the laser must have a wide tuning range, and highest possible average power during the X-ray FEL pulse train.

For applications in the visible and near-visible wavelength range a pump-probe facility based on a conventional quantum laser system will be available at the TTF [3] (see Fig. 1). The laser system comprises a seed pulse laser, special synchronization with the accelerator, pulse shaping, and a pump laser together with an optical parametric amplifier (OPA).

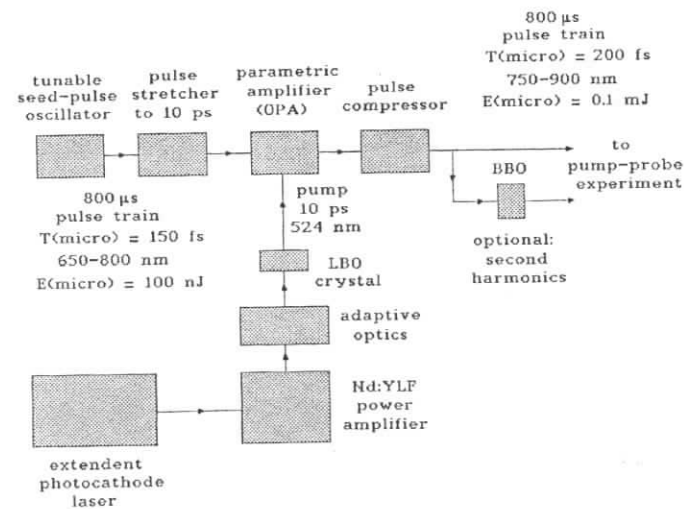


Fig. 1. Basic scheme of the conventional laser system

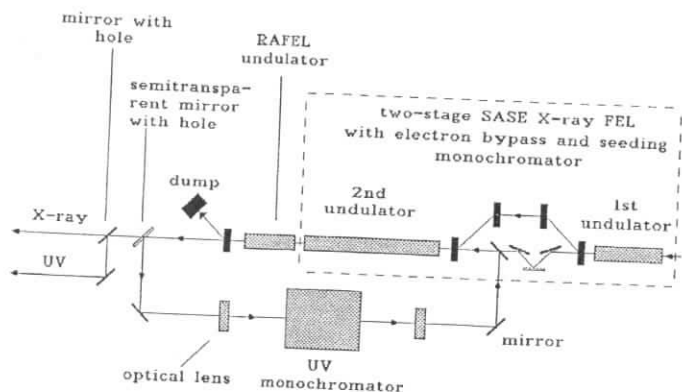


Fig. 2. Schematic layout of the pump-probe facility combining UV regenerative FEL amplifier and soft X-ray FEL at TTF

The laser will provide in the visible spectral region between 750 and 900 nm a train of 150 fs pulses with 100  $\mu\text{J}$  of optical energy per pulse, at the same repetition rate as the X-ray FEL. This requires the development and construction of an OPA, pumped by a unique, frequency doubled Nd:YLF laser with 10 ps pulse length and 3 kW average power during the ms pulse train. Grating combinations will be used to adopt the duration of the seed-pulses to the pulse duration of the pump laser and recompress them after parametric amplification (CPA Chirped-Pulse Amplification). Briefly, the main technical problems of this project are the development of the high power OPA and the synchronization system. The synchronization of the optical laser with the soft X-ray FEL pulses to within 200 fs is the most challenging task of this project. The main problem is the time jitter ( $\pm 1$  ps) of electron bunches which are synchronous with the soft X-ray FEL pulses.

In this paper we describe the extension of the pump-probe facility into the ultraviolet wavelength range. Our approach is based on the idea to use a narrow band feedback between exit and entrance of a high gain FEL amplifier operating in multibunch mode (so called regenerative FEL amplifier - RAFEL [4]). Such a feedback can be realized in the UV wavelength range using mirrors, lenses, and a dispersive element. We propose to install an additional 6 m long undulator (magnet period length  $\lambda_w = 7$  cm, the maximum value of the magnetic field is about 1.4 T) after the soft X-ray FEL. A layout of the proposed RAFEL is shown in Fig. 2. This design makes use of the spent electron beam leaving the X-ray undulator. The SASE process in the X-ray FEL induces an additional energy spread in the electron beam. Nevertheless, the electron beam at the exit of the X-ray FEL is still a good "active medium" for an UV FEL amplifier. The motivation for this approach was to meet the user requirement for precise synchronization of pump and probe

pulses. The proposed scheme possesses significant advantages. Since it is a single bunch scheme, it does not require any special synchronization. It reveals a perspective to achieve synchronization close to the duration of the radiation pulses (200 fs). Because the RAFEL uses the spent electron beam, the proposed laser system operates in a "parasitic" mode not interfering with the main mode of the X-ray FEL operation. The RAFEL proposed here will provide intense, tunable and coherent radiation in the UV region of the spectrum between 200 and 400 nm as direct laser output. The RAFEL output radiation has the same pulse format as the X-ray FEL and produces 200 fs micropulses with 2 mJ of radiation energy per micropulse and transform-limited spectral width.

The narrow band feedback optical system needed for the RAFEL scheme basically has to satisfy two requirements. First, it has to cut out a narrow band of the radiation from the SASE spectrum, covering the full spectral range of the FEL amplifier. Second, the selected narrow-band photon pulse must fully overlap the electron bunch at the entrance of the radiation  $\Delta\lambda/\lambda$  at the entrance of the undulator should be less than  $\lambda/(\pi\sigma_z)$ , where  $\sigma_z$  is the rms length of the electron bunch. In this case the monochromatic photon pulse and electron bunch would have the same length providing optimum seeding efficiency. The main problem of constructing a RAFEL at the TTF is the time jitter of the input electron beam pulses. In our case the 0.2 ps long photon pulse should be stretched, i.e. the monochromator bandwidth should be further reduced, in order to avoid a reduced overlap between electron and photon pulses due to a  $\pm 1$  ps time jitter. This requires a resolving power of the monochromator  $\lambda/\Delta\lambda \simeq 6000$  at  $\lambda = 200$  nm.

The main goal of the present study has been to design a pump-probe facility which is compatible with the layout of the TTF and the X-ray FEL under construction at DESY, and which can be realized with minimal additional efforts. The RAFEL undulator and outcoupling optical system proposed can be installed in the unoccupied straight vacuum line used to transfer the X-ray beam to the experimental area, behind the dipole magnet separating the electron beam from the X-ray beam. The installation of the feedback is greatly facilitated by the fact that there is free space available for the input optical system. In order to get fully coherent X-ray radiation, a seeding option will be implemented into the X-ray FEL under construction at DESY [5]. The X-ray FEL seeding option consists of an additional 18 m long undulator, an electron bypass and X-ray grazing incidence monochromator (see Fig. 2). The electron bypass is necessary to delay the electron beam by the same amount as the X-ray photon beam is delayed by the X-ray monochromator. The magnetic chicane has to deflect the electron beam out of the straight flight pass to make room for the X-ray monochromator and input optical elements of RAFEL.

## 2 Facility description

The RAFEL parameters are presented in Table 1. The RAFEL operates as follows. The first bunch in a train of up to 7200 bunches amplifies shot noise and produces intense, but wide-band radiation. A fraction of the radiation is back-reflected by a semi-transparent output coupling mirror. The spherical grating which is installed in the straight section of the feedback loop, disperses the light and focuses a narrow band of radiation back on the entrance of the undulator. The bandwidth of the feedback is chosen to produce a photon pulse length about ten times as long as the electron bunch length in order to avoid effects from a  $\pm 1$  ps time jitter. This requires a resolving power  $\lambda/\Delta\lambda \simeq 6000$  at  $\lambda = 200$  nm (photon pulse duration at the monochromator exit  $t_{ph} \simeq \lambda^2/(c\Delta\lambda) \simeq 4$  ps).

If the optical pass length between output coupling mirror and input mirror is properly adjusted, the monochromatic photon pulse coming from the first electron bunch in the train travels together with the fifth electron bunch. The peak of the reflected radiation pulse of 4 ps duration can be easily tuned to the arrival time of the short electron bunch at a predicted absolute jitter of about one picosecond (see Fig. 3). Calculations show that an alignment accuracy of about  $10 \mu\text{rad}$  is sufficient for reliable operation of the optical feedback.

After the undulator the electron and the radiation beams are separated. The electron beam is guided into the beam dump and the radiation enters the output coupling system. The distance between the feedback outcoupling mirror and the exit of the the RAFEL undulator is 20 m, the distance between the mirror and the exit of the X-ray FEL undulator is about 27 m. The minimum size of the hole in the outcoupling mirror is defined by the condition that X-ray radiation losses due to hole aperture limitation should be avoided.

Table 1. Parameters of the UV pump-probe facility (RAFEL option)

<u>Electron beam</u>	
Energy	1000 MeV
Charge per bunch	1 nC
rms bunch length	50 $\mu\text{m}$
rms normalized emittance	2 $\pi$ mm mrad
rms (VUV FEL induced) energy spread	2.5 MeV
Number of bunches per train	7200
bunch spacing	111 ns
Repetition rate	10 Hz
<u>Undulator</u>	
Type	Planar (permanent)
Period	7 cm
Peak magnetic field	1-1.4 T
Number of periods	85
<u>Output radiation</u>	
Wavelength	200-400 nm
Bandwidth	Transform-limited
micropulse duration	200 fs
micropulse energy	4 mJ
bunch spacing	111 ns

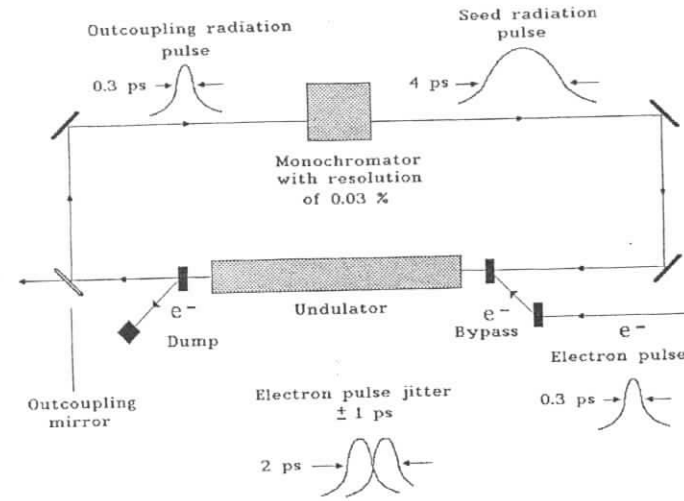


Fig. 3. The use of a monochromator as a pulse stretcher. Drawing illustrates how electron pulse jitter effects on the feedback system can be avoided

The fraction of the output the X-ray FEL power passing the mirror hole is calculated from the angular distribution of the X-ray radiation (20  $\mu\text{rad}$  rms). At a diameter of the hole in the mirror of 3 mm the fraction of the X-ray power directed through the mirror is close to 100%. This mirror is semi-transparent for the UV radiation, and approximately 50% of the UV radiation power is transmitted through it and delivered to the experimental area.

The monochromator for the RAFEL should be able to select any wavelength between 200 and 400 nm. The optics needed to couple the radiation in and out of the monochromator would be particularly simple and symmetric if a monochromator design was chosen whose magnification would be independent of wavelength. Therefore, a Rowland circle grating monochromator appears to be ideal suited for this purpose since the magnification of the spherical grating is always unity, independent of wavelength. The specific design of a monochromator at normal incidence with a curved grating is shown in Fig. 4. We adopted the Namioka scheme where tuning of the wavelength is performed by means of rotation of the grating, while entrance and exit slits are fixed. Commercially available holographic gratings allow one to focus the image of the entrance slit exactly on the exit slit at small values of coma and astigmatism in the 200-400 nm wavelength band. For a Namioka grating configuration, the rms pulse stretching per grating reflection is calculated to be  $w_{st} \simeq \lambda w_x/d$ , where  $w_x$  is the radiation beam size at the grating and  $d$  is

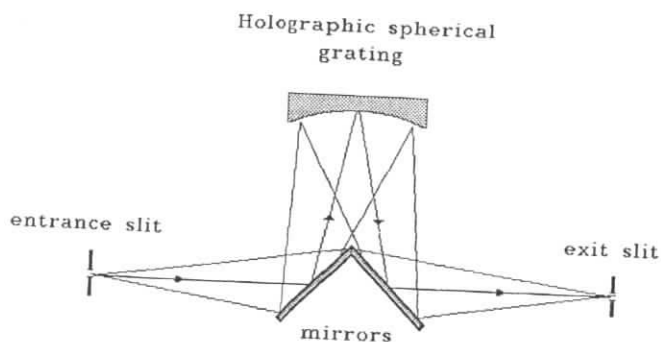


Fig. 4. Optical arrangement for the feedback system monochromator

the groove spacing. To avoid a gain instability,  $w_{st}/c$  should be large compared with the electron pulse jitter ( $\pm 1$  ps).

The feedback transmission factor can be written as  $T_{fb} = K_{coupl} \times R_{loss}$ , where  $K_{coupl}$  is the fraction of output radiation coupled out through the semi-transparent mirror,  $R_{loss}$  refers to the losses in the optical elements (mirrors, lenses, grating) of the feedback system. In addition, the grating reduces the peak power of the coherent signal further since it stretches the pulse longitudinally by a factor  $\lambda^2/(\sigma_z \Delta \lambda)$  [6].

In the present design the lateral size of the photon beam focus,  $w$ , is completely determined by the fixed geometry of the feedback optical system (i.e. the focal distances of the mirrors and the aperture of the X ray undulator vacuum chamber). In our numerical example for 400 nm wavelength the size of the photon beam focus is about  $w \simeq 800 \mu\text{m}$ , which is about 15 times larger than the rms electron beam size,  $\sigma$ . Such a mismatch, however, is not dramatic and will result in a reduction of the gain by a factor of about 3 only (see section 3 for more details).

Taking into account all the effects mentioned above, the overall loss factor for the feedback system is about  $2 \times 10^{-2}$ . When the power gain in the undulator,  $G$ , exceeds the relative losses of power in the optical feedback system, the output radiation power begins to grow, i.e. lasing takes place. The undulator is one of the central components of the RAFEL. It has to provide the sinusoidal field, so that the FEL process can take place. The values of the peak field and the period length are given in Table 1. The required field strength can be achieved using a hybrid configuration. The term "hybrid" means that soft iron pole pieces are used in conjunction with Nd-Fe-B permanent magnets. At a gap of 12 mm, a peak field up to 1.5 T is feasible for the undulator period of  $\lambda_u = 7$  cm. This is more than needed for the RAFEL undulator. It is shown in section 3 that the maximum

value of the gain well exceeds the relative losses of peak power in the optical feedback system when the undulator is at least 6 m long.

In this section we present a specific numerical example for the regenerative FEL amplifier operating at the wavelength of 200 nm. However we would like to emphasize that the wavelength can be tuned continuously by changing the undulator magnetic field and adjusting the monochromator wavelength by simple rotation of the grating. Using the present design it should be possible to cover the range from 200 nm down to 400 nm. The FEL wavelength is given by

$$\lambda = \frac{\lambda_w(1 + K^2/2)}{2\gamma^2}$$

where  $\lambda_w$  is the period length of the undulator magnet,  $\gamma$  is the electron's relativistic energy  $\mathcal{E}$  divided by its rest energy  $m_0c^2$ , and  $K$  is the dimensionless undulator parameter, related to the peak magnetic field  $H_w$  in the undulator and the electron charge  $e$  as follows:

$$K = \frac{eH_w\lambda_w}{2\pi m_0c} = 0.934H_w[T]\lambda_w[\text{cm}].$$

From these relations, it is clear that the FEL wavelength can be changed either by changing the electron beam energy or by changing the undulator magnet gap (thereby changing  $K$ ). We suppose to change the undulator gap for tuning the wavelength within the 200–400 nm range, since the choice of the electron energy is dictated by the X-ray FEL. At a fixed electron energy  $\mathcal{E}$ , the wavelength can be varied between  $\lambda_{min}$  and  $\lambda_{max}$ , where

$$\frac{\lambda_{max}}{\lambda_{min}} = \frac{1 + K_{max}^2/2}{1 + K_{min}^2/2} = 2.$$

Thus, for the chosen undulator period length (7 cm) and maximum wavelength (400 nm) the maximum value of undulator parameter is  $K_{max} = 9.3$ . The corresponding peak magnetic field on the undulator axis is 1.4 T. The minimal gap corresponding to  $K_{max}$  is  $g_{min} = 13$  mm.

The minimum value of  $K$ , obtained by opening the gap, was chosen as  $K_{min} = 6.5$ . The dependence of the undulator parameter on the magnet gap is given approximately by

$$K = K_{max} \exp\left[-\frac{\pi(g - g_{min})}{\lambda_w}\right].$$

Thus, the maximum gap corresponding to  $K_{min} = 6.5$  is  $g_{max} = 18$  mm.

The soft X-ray FEL facility will be realized at DESY after a proof of SASE principle experiment for wavelengths from about 70 to 120 nm (Phase I). During this phase the linear accelerator will operate at electron beam energies up to 300 MeV. In Phase II of the project the accelerator will be extended to increase the electron beam energy to more than one GeV and to drive a FEL facility down to wavelengths of a few nanometers [1, 2].

It should be noted that there are similarities between our RAFEL design for pump-probe experiments and the VUV RAFEL which will be installed at the end of the first stage of the TTF FEL project [7]. The distance between optical elements of the VUV RAFEL (66.4 m) is equal to those required in the present design. The bandwidth of the VUV RAFEL feedback system is chosen to produce a photon pulse length of about 4 ps in order to avoid effects from the same time jitter. Comparing the parameters of the VUV RAFEL with the present design we can conclude that it will be more difficult to achieve lasing in the case of the VUV RAFEL. On the one hand, the wavelengths of the VUV radiation are four times smaller compared with our present design and the alignment accuracy of the VUV RAFEL optical system is about  $2 \mu\text{rad}$ . On the other hand, in the present case the required resolution of the monochromator can be achieved without significant efforts. There is also a highly developed technology of optical elements (lenses, holographic gratings, fast electrooptical switches, semi-transparent plates, etc.) operating in the visible and UV wavelength range. This means that a successful operation of the VUV RAFEL at the TTF would prove that the required stability of the optical system and the accelerator are feasible.

### 3 Operation of the regenerative FEL amplifier

Normally it is assumed that the electron beam should be dumped after leaving the undulator that produces the X-ray radiation. The quality of this spent beam is too low for the generation of short wavelength radiation, but it can still be used for driving an FEL operating at longer wavelengths. Our study has shown that the spent electron beam can drive FEL amplifier operating at 50 nanometers or longer wavelength. However, in the framework of the present design of the TESLA Test Facility there are severe limitations of free space available after the X-ray undulator which can be used for installing additional hardware. A single-pass UV SASE FEL would require a length of about 20 meters, which is out of space available at the TTF. A regenerative FEL amplifier is a natural solution to reduce the required length. As mentioned above, RAFEL will work when the single pass gain in the undulator exceeds the power losses in the feedback optical system. In the case under study (UV wavelength band, 200–400 nm), the single pass gain must be higher than 50. To minimize the length of the matching section between the VUV/X-ray undulator and RAFEL undulator, we decided to use the same value of the beta function of 3 meters. The value of the undulator period has been chosen equal to 7 cm which is optimal for the amplification of radiation in the 200–400 nm wavelength band.

We begin our study with the analysis of physical effects influencing the operation of the FEL amplifier. Within the scope of the three-dimensional theory of the FEL amplifier

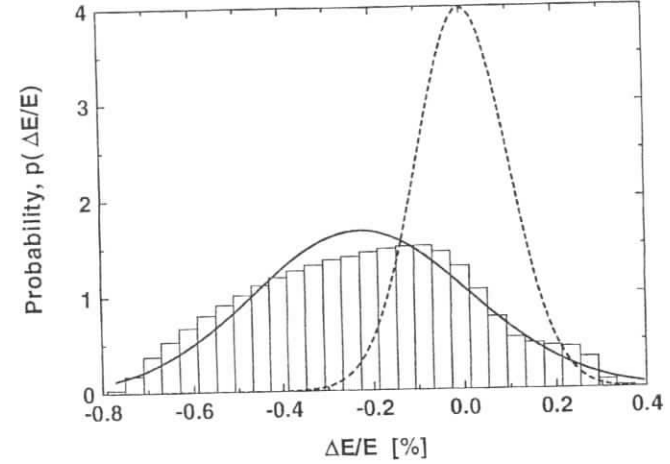


Fig. 5. Histogram of energy distribution of the particles after leaving the VUV/X-ray FEL driven by 1 GeV electron beam. The solid line represents a Gaussian distribution with the rms deviation  $\sigma_E = 2.5 \text{ MeV}$ . The dashed line is the energy distribution at the entrance of the VUV/X-ray undulator ( $\sigma_E = 1 \text{ MeV}$ )

we obtain that all the important physical effects are connected with the corresponding dimensionless parameters: the diffraction parameter  $B$ , the space charge parameter  $\hat{A}_p^2$ , the parameter of the longitudinal velocity spread  $\hat{A}_1^2$  and the efficiency parameter  $\rho$  [9]:

$$\begin{aligned}
 B &= 2\Gamma\sigma_r^2\omega/c \\
 \hat{A}_p^2 &= A_p^2/\Gamma^2 = 4c^2(\theta_s\sigma_r\omega A_{JJ})^{-2}, \\
 \hat{A}_1^2 &= A_1^2/\Gamma^2 = (\sigma_E^2/\epsilon_0^2 + \gamma_z^4\sigma_\theta^4/4)/\rho^2, \\
 \rho &= c\gamma_z^2\Gamma/\omega.
 \end{aligned} \tag{1}$$

The gain parameter  $\Gamma$  defines the scale of the field gain and is defined as

$$\Gamma = [IA_A^2\omega^2\theta_s^2/(2I_A c^2\gamma_z^2\gamma)]^{1/2}, \tag{2}$$

where  $\omega = 2\pi c/\lambda$  is the frequency of the radiation field,  $I$  is the beam current, and  $I_A = m_e c^3/e$ . To be specific, we have written all the formulae for the case of a Gaussian distribution of the electrons in the transverse phase space with the RMS radius and the RMS angular spread given by  $\sigma_r = \sqrt{\epsilon_n\beta/\gamma}$  and  $\sigma_\theta = \sqrt{\epsilon_n/\beta\gamma}$ , respectively, where  $\epsilon_n$  is rms normalized emittance, and  $\beta$  is the focusing beta function. The energy spread in the electron beam is assumed to be Gaussian with the rms deviation  $\sigma_E$ . The undulator is assumed to be planar with amplitude of the magnetic field  $H_w$  and period  $\lambda_w$ . The angle of electron oscillations  $\theta_s$ , the longitudinal relativistic factor  $\gamma_z$  and the factor  $A_{JJ}$  are defined

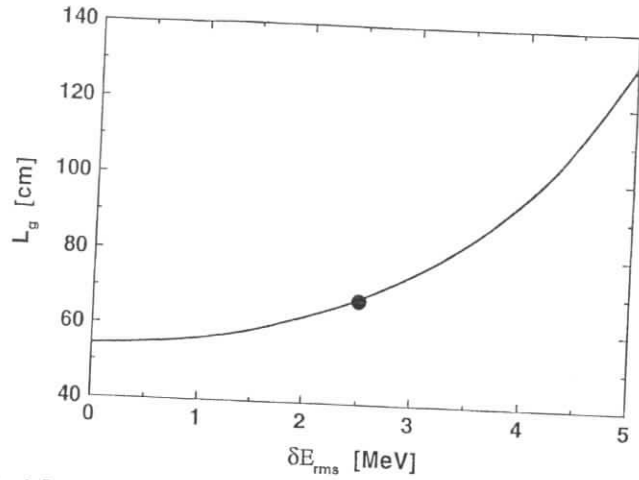


Fig. 6. Power gain length,  $L_g$ , versus energy spread in the electron beam for the operation of the FEL amplifier at the wavelength of 200 nm.

Table 2. Dimensionless parameters for RAFEL

	200 nm	300 nm	400 nm
Diffraction parameter, $B$	0.21	0.14	0.1
Space charge parameter, $\hat{A}_p^2$	0.24	0.36	0.48
Parameter of longitudinal velocity spread, $\hat{A}_T^2$		0.086	
Efficiency parameter, $\rho$		0.006	

as follows:  $\theta_s = K/\gamma$ ,  $\gamma_z^2 = \gamma^2/(1+K^2/2)$  and  $A_{JJ} = J_0(K^2/(4+2K^2)) - J_1(K^2/(4+2K^2))$ , where  $J_0$  and  $J_1$  are the Bessel functions.

The corresponding values of the dimensionless parameters for operation of the RAFEL at different wavelengths are summarized in Table 2. The value of the gain parameter is almost constant,  $L^{-1} \simeq 93$  cm, for all wavelengths. The parameter of the longitudinal velocity spread  $\hat{A}_T^2$  was calculated using actual energy distribution in the electron beam after leaving the VUV/X-ray undulator (see Fig. 5). It is seen that the distribution function of the electrons can be fitted well by a Gaussian distribution with the rms deviation  $\sigma_E \simeq 2.5$  MeV.

It is seen that the main physical effects defining the operation of the FEL amplifier are the diffraction effects and the space charge effects. Since the value of  $\hat{A}_T^2$  is small, we can state that the energy spread does not influence too much the gain at chosen parameters of the FEL amplifier. The numerical solution of the corresponding eigenvalue equation [9] confirms this simple physical consideration (see Fig. 6). It is seen that the power gain length is increased by 20% only with respect to the case of a "cold" electron beam.

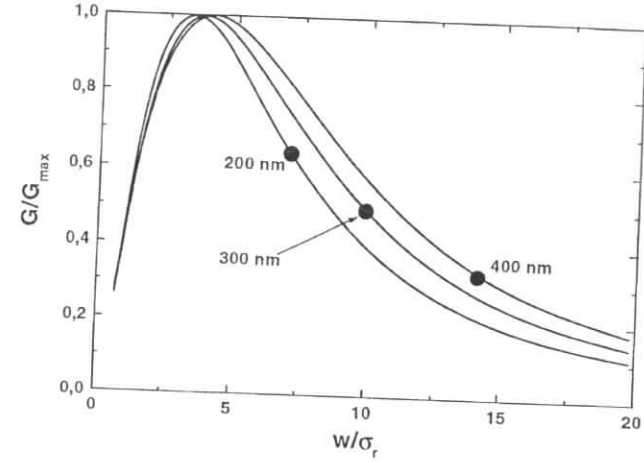


Fig. 7. Power gain in the linear regime versus spot size of the seeding radiation beam (the rms transverse size of the electron beam is  $\sigma_r = 55 \mu\text{m}$ )

Using the plot presented in Fig. 6 we can estimate that about nine power gain lengths,  $L_g$ , fit in the 6 meters long undulator. Calculations of the total power gain must take into account the details of focusing of the external radiation on the electron beam at the undulator entrance. A quantitative description may be performed in the following way. We assume that the seed radiation has a Gaussian radial intensity distribution which is characterized by the position of the focus,  $z_0$ , and the size of the waist in the focus,  $w$ . In the high-gain linear (steady-state) regime the radiation power grows exponentially with the undulator length:

$$G = P_{\text{out}}/P_{\text{in}} = A \exp[z/L_g],$$

where  $P_{\text{out}}$  and  $P_{\text{in}}$  is the output and input power, respectively. The input coupling factor  $A$  depends on the focusing of the seed radiation and is a function of  $z_0$  and  $w$ . It should be maximized by an appropriate choice of  $w$  and  $z_0$ . This problem has been studied in detail in [9] using the solution of the initial-value problem. It has been found that the value of  $A$  at  $z_0 = 0$  does not differ significantly from its maximal value and the position of the Gaussian beam waist can be placed at the coordinate of the undulator entrance. However, due to the constraints of the present design we have no possibility to achieve the optimal value by using the focusing optics. The reason for this is that the focusing mirror can only be placed at a fixed position of 20 meters apart from the RAFEL undulator entrance. Also, there is an aperture limitation of 9 mm due to the diameter of the vacuum chamber in the VUV/X-ray undulator. These constraints lead to the minimum sizes  $w$



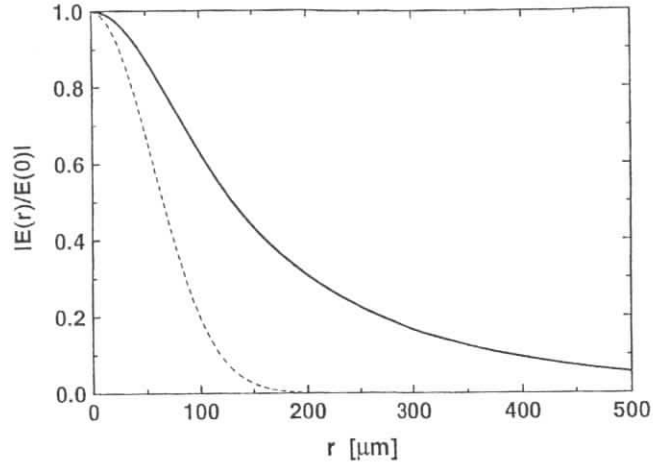


Fig. 8. Transverse distribution of the radiation field amplitude for the FEL amplifier operating at a wavelength of 200 nm. The dashed line is the transverse profile of the electron beam current density,  $\exp[-r^2/(2\sigma_r^2)]$  with  $\sigma_r = 55 \mu\text{m}$

of the seeding optical beam at the entrance of the RAFEL undulator of 400, 600, and 800  $\mu\text{m}$  for the wavelengths of 200, 300, and 400 nm, respectively. Fortunately, this does not lead to significant degradation of the gain as it is illustrated in Fig. 7. In the worst case (operation at 400 nm) the gain degrades only by a factor of three with respect to the optimal case. The reason for this is the strong influence of diffraction effects. In the general case the seeding radiation should be matched with the beam radiation mode, but not with the transverse size of the electron beam. In the case of small diffraction parameter, the transverse size is larger than the transverse size of the electron beam as it is illustrated in Fig. 8.

Figure 9 presents the plots for the power gain,  $G = P_{\text{out}}/P_{\text{in}}$  versus undulator length for the FEL amplifier operating in the linear regime at 200 and 400 nm wavelength. The radiation beam size at the undulator entrance  $w$  is equal to 400 and 800  $\mu\text{m}$  for 200 and 400 nm operating wavelength, respectively. It is seen that the gain only slightly depends on the wavelength for an undulator length of 6 meters. The reason for this is the specific problem of focusing the radiation, it becomes less optimal at increasing wavelength (see Fig. 7). On the other hand, the power gain length decreases with the increase of the wavelength. At a relatively short undulator length these two effects compensate each other.

The final optimization of the FEL amplifier parameters has been performed with the nonlinear, three dimensional, time-dependent simulation code FAST [8]. The optimized

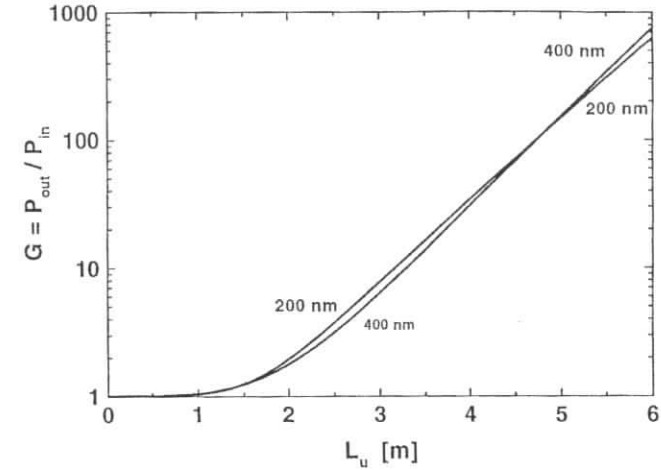


Fig. 9. Power gain,  $G = P_{\text{out}}/P_{\text{in}}$  versus undulator length for the FEL amplifier operating at 200 and 400 nm wavelength (radiation beam size at the undulator entrance  $w$  is equal to 400 and 800  $\mu\text{m}$ , respectively)

parameters of the FEL amplifier are presented in Table 1. Fig. 10 presents the evolution of the energy in the radiation pulse along the undulator. Fig. 11 shows the time structure of the radiation pulse at the exit of the undulator. We obtain that the RAFEL operating at saturation produces 4 mJ pulses of about 200 fs pulse duration. Figure 12 shows the spectral distribution of the radiation power at the exit of the RAFEL undulator.

The analysis of the RAFEL parameters has shown that it will operate reliably even at a value of the energy spread exceeding the project value for the TTF by a factor of two. There is also a safety margin (by a factor of two) with respect to the value of the emittance. Therefore, we can conclude that the RAFEL at the TTF (Phase II) will operate reliably with large safety margins with respect to critical parameters of the accelerator.

#### Acknowledgments

We thank D. Trines and J.R. Schneider for their interest in this work and their support.

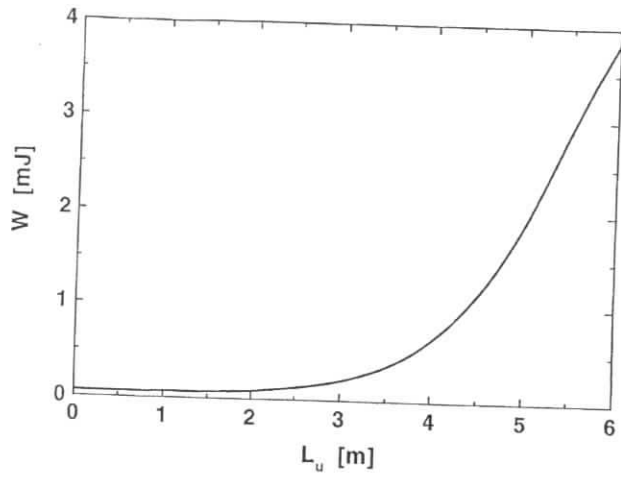


Fig. 10. Energy in the radiation pulse versus undulator length for the RAFEL operating at the wavelength of 200 nm

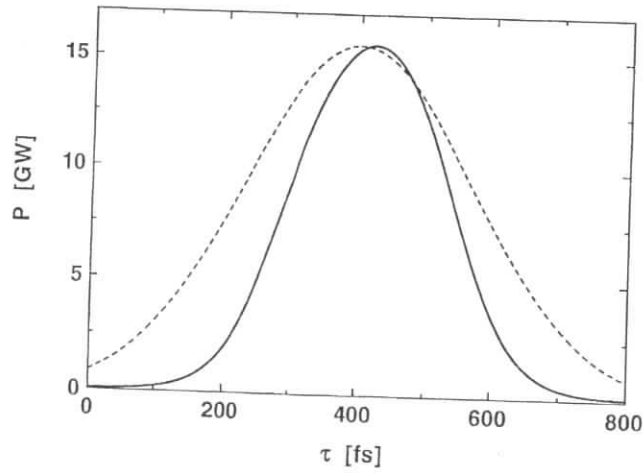


Fig. 11. Temporal structure of the radiation pulse at the exit of the RAFEL undulator. The dotted line represents the longitudinal profile of the electron beam current (the maximum corresponds to 2.5 kA)

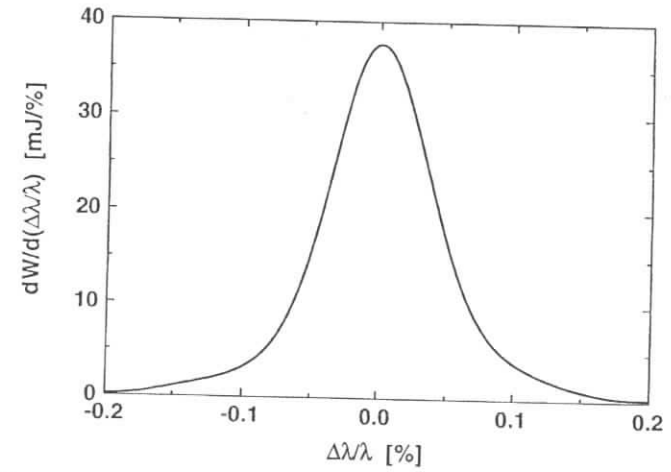


Fig. 12. Spectral structure of the radiation pulse at the exit of the RAFEL undulator

## References

1. "A VUV Free Electron Laser at the TESLA Test Facility: Conceptual Design Report", DESY Print TESLA-FEL 95-03, Hamburg, DESY, 1995
2. J. Rossbach, Nucl. Instrum. and Methods A 375(1996)269
3. "Development of a pump-probe facility with sub-picosecond time resolution combining a high-power optical laser and a soft X-ray free electron laser": Joint DESY (Germany), Forschungszentrum Julich (Germany), Max-Born-Institute Berlin (Germany), Dublin City University (Ireland), MAX-Lab/Lund Laser Centre (Sweden) and CNRS/LURE, Orsay (France) Proposal. Available at DESY by request only
4. J. Goldstein, D. Nguyen and R. Sheffield, Nucl. Instrum. and Methods A 393(1997)137
5. "Seeding Option for the VUV Free Electron Laser at DESY": Joint DESY and GKSS Proposal. Available at DESY by request only
6. J. Sollid et al., Nucl. Instrum. and Methods A 285(1989)147
7. B. Faatz et. al., Nucl. Instrum. and Methods A 429(1999)424
8. E. L. Saldin, E. A. Schneidmiller, and M.V. Yurkov, Nucl. Instrum. and Methods A 429(1999)233
9. E. L. Saldin, E. A. Schneidmiller, and M.V. Yurkov, "The Physics of Free Electron Lasers" (Springer-Verlag, Berlin-Heidelberg-New-York, 1999)

